Pavement Condition Measurement at High Velocity using a TSD

A. Malekjafarian
University College Dublin, Ireland

D. Martinez
University College Dublin, Ireland; Greenwood Engineering, Denmark

E. J. OBrien
University College Dublin, Ireland

ABSTRACT: The aim of this paper is to present the latest developments in the use of an instrumented vehicle called the Traffic Speed Deflectometer (TSD). A large axle load is applied to the pavement under the TSD. The deflection caused by this axle load is measured using several Doppler lasers. In the first step, the velocity of the deflection of the pavement is measured which can be shown to be proportional to the slope of the deformed profile. The pavement deflection is calculated in the second step using an integration model. A Winkler model is used to simulate the pavement behaviour under the axle load and the TSD is represented as a half-car model. The TSD is shown to be an effective tool for pavement damage detection.

1 INTRODUCTION

Pavement condition monitoring techniques have been used for many years. Visual inspection (de Velasco and McCullough, 1983) is still used for quick assessment, but it just works in easily-seen pavement damage situations such as visible cracks or subsidences. Despite its effectiveness, only a rough estimation of the damage can be done and a change in the pavement damage may not be visible. In these situations, a more reliable technique is necessary.

Sampling taking some parts of the pavement is one of the earliest methods that has been used for the analysis of pavement condition (Shahin and Walther, 1990), but there are several issues. Firstly, some parts of the pavement need to be removed. It is also impractical to assess the entire road in this way. Systematic sampling (Shahin and Kohn, 1981) has been suggested in which several samples at a defined distance are taken from the road. Although this method may provide more reliable data about the pavement condition, it causes more damage to the pavement.

Pavement monitoring using a passing vehicle is proposed and these vehicles are referred as Non-Destructive Testing (NDT) devices (Davies and Mamlouk, 1985) as material extraction is not required. The Benkelman beam, Dynaflect, Road Rator and Falling Weight Deflectometer (FWD) are the best known NDT devices (Davies and Mamlouk, 1985). Of these, FWD is the most common device for pavement stiffness measurement and it has several advantages compared to the other methods (Chang et al., 2002). It measures deflections on the surface of the pavement due to the dropping of a known mass (Yi and Mun, 2009). Load cells and velocity transducers are used for the measurements (Roesset and Shao, 1985). The key problem with the FWD is that it is stationary when in operation so it obstructs the traffic and creates safety issues (Rada et al., 2015). Continuous Deflection Devices (CDDs) have been introduced to solve this problem (Katicha et al., 2014a). CDDs measure deflection at driving speed, avoiding the safety implications of stationary measurements (Katicha et al., 2014b). The two main CDDs are the Rolling Weight Deflectometer (RWD) and the Traffic Speed Deflectometer (TSD). RWD uses several lasers to measure the deflection. The deflection under the tyre is obtained using the principle of triangulation (Johnson et al., 1996). In a TSD, Doppler lasers are used for measuring the velocity of the deflection. The deflections are calculated by post-processing of the measured velocities (Rasmussen et al., 2002).

Deflection can be inferred using two different approaches: numerical integration or model calibration. Model calibration uses the model of the deflection basin in order to fit the slope measurements to the deflection values. The deflection basin model is a function composed of several parameters. The greater the number of parameters involved, the better the accuracy in deflection results. Pavement deflections are the final outputs of the TSD. Much research has been done to infer damage in pavements from measured deflections (Donovan and Tutumluer, 2009). However, there are many discussions regarding the accuracy of these methods (Gopalakrishnan and Khaitan, 2010).

A pavement condition assessment method can be developed by correlating the TSD deflection data with data obtained using a FWD. Chai et al. (2016) analyses a section of pavement with both an FWD and a TSD, establishing a correlation between them. Donovan and Tutumluer (2009) state that the shape of the deflection basin can provide information about the quality of the pavement layers. Based Damage Index (BDI) and Based Curvature Index (BCI) are proposed by (Xu et al., 2002) to measure damage related to loss of stiffness.

Pavement Layer Moduli Backcalculation (PLMB) is one of the most popular techniques to calculate damage from deflection. Some numerical procedures are available with computationally intensive calculations as an iteration process is needed (Chou and Lytton, 1991). Three main parameters can be highlighted in the simulation of the pavement for PLMB: Elastic modulus, layer thickness and Poisson's ratio. Poisson's ratio is usually estimated and elastic modulus is calculated, providing damage information. PLMB can be applied for static or dynamic loads with a linear or a non-linear approach (Von Quintus and Killingsworth, 1997).

This paper explains how pavement deflection is calculated from the relative velocity measured in a TSD. A Winkler model approach is used to simulate the pavement and a Half-Car model is used to represent the TSD characteristics. The pavement deflection calculated from the numerical model is compared with the experimental results obtained from an asphalt road. Fatigue damage is added in the Winkler model and compared to the undamaged simulation. It is shown that real TSD behaviour can be modelled with a simple one layer Winkler model considering mainly the pavement stiffness.

2 TRAFFIC SPEED DEFLECTOMETER OPERATION

A TSD includes three main parts: the trailer, the Doppler lasers and the beam.

2.1 *The trailer*

A TSD is mainly a truck as shown in Figure 1 which includes the axle load on the pavement and most of the equipment. Axle load can vary depending on the circumstances. The indoor temperature of the trailer is kept constant to avoid contraction or dilatation of the beam. Measurements can be taken at a maximum driving speed of 80 km/h.

2.2 *The beam*

The beam is made of steel and its function is to ensure that the components are in the correct position. This beam is equipped with accelerometers, gyrocopes and the Doppler lasers. The beam is always kept parallel to the road using the data measured on it. For this reason, translation and rotation are allowed in the beam.

Figure 1. Greenwood TSD

2.3 *The Doppler lasers*

Several Doppler lasers are installed on the beam which measures the relative deflection velocity between it and the pavement (Fig. 2). The first laser is called the reference laser and it is placed between the two axles. All Doppler lasers are installed on the beam at specified intervals, depending on the TSD model. The Doppler Effect is used for measuring the relative velocity as Doppler lasers are both emitter and receiver. The change in the frequency of the input signal allows the calculation of the relative velocity between the beam and the pavement.

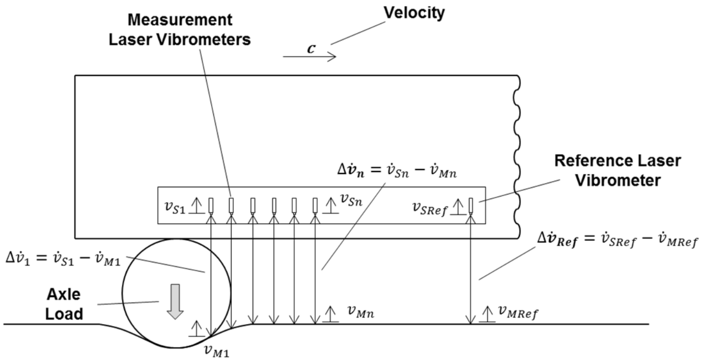

Figure 2. Laser positions on the beam and deflection basin caused by axle load.

3 SLOPE CALCULATION

The deflection slope is obtained through the deflection velocity measurements. This process involves some corrections to ensure the highest accuracy possible. Translation and rotation of the beam are two sources of inaccuracy. The translation error is related to the substantially vertical velocity of the beam and it has the same influence on all the measurements taken from the Doppler lasers. This error is eliminated by simply subtracting the relative velocity of the reference sensor from the measuring sensors in the region of the deflection basin. The error caused by the beam rotation is corrected using the rotational velocity directly measured by the gyroscope. The relative velocity between the reference laser and a measuring laser caused by the beam rotation, is calculated as:

$$\Delta\dot{v}_{Beam} = \Delta\omega_{\ddot{u}} \times x \quad (1)$$

where $\Delta\omega_{\ddot{u}}$ is the rotational velocity of the beam and x is the distance between the measuring sensor and the reference one. It is assumed there is no load and therefore no deflection in the pavement under the reference laser. This means that the relative velocity measured at the reference laser is composed of the translational velocity and the velocity resulting from the rotation of the beam.

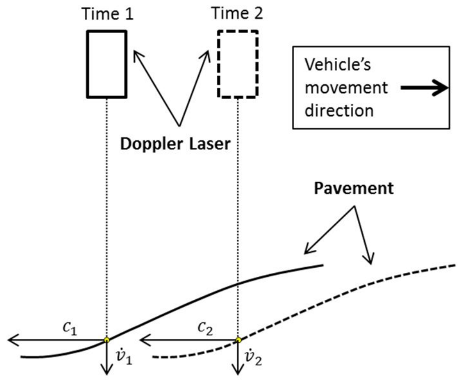

Figure 3. Velocity components measured in TSD operation.

The two components of the velocity are shown in Figure 3: the vertical and the horizontal. The horizontal component is defined by the velocity of the vehicle c. Direction of horizontal velocity of the vehicle in the pavement is the opposite as the basin is moving with the wheel. The vertical velocity is related to the vertical deflection v caused by the TSD's load:

$$\dot{v} = \frac{\Delta v}{\Delta t} \quad (2)$$

Same analogy can be resolved for vehicle's velocity that can be expressed as a function of the horizontal deflection u:

$$c = \frac{\Delta u}{\Delta t} \quad (3)$$

An implication of this is the possibility that slope α is calculated using velocities differentiating from the basic slope formula with deflections.

$$\alpha = \frac{v}{u} = \frac{\dot{v} \times \Delta t}{c \times \Delta t} = \frac{\dot{v}}{c} \quad (4)$$

The slope at the point the laser is measuring is the ratio between velocity of deflection and the driving speed. The slope is calculated using the velocity calculated from beam rotational velocity in Eq. 1, the reference sensor velocity and the measuring sensor velocity. Substituting the vertical velocity in Eq. 4 slope is calculated:

$$\alpha = \frac{\Delta\dot{v}_n - \Delta\dot{v}_{Ref} - \Delta\dot{v}_{Beam}}{c} \quad (5)$$

where $\Delta\dot{v}_n$ is the velocity measured by the Doppler laser sensor on the deflection basin, $\Delta\dot{v}_{Ref}$ is the velocity measured by the reference laser and $\Delta\dot{v}_{Beam}$ is the velocity obtained using the gyroscope. $\Delta\dot{v}_{Ref}$ removes the error caused by beam's translation, considering that the slope at that point should be zero and therefore a zero velocity has to be measured. A full measurement of the error is performed with the reference laser.

4 WINKLER MODEL NUMERICAL SIMULATION

A Winkler model is used to represent the pavement. This model uses a beam supported by many springs separated by a constant distance. The springs and the beam stiffness represent the whole stiffness of the pavement. Stiffness is the main parameter in the analysis of pavement in this model. An asphalt road structure is considered as it is the most used. The TSD is simulated as a longitudinal Half-car model with 4 degrees of freedom (DOFs). This longitudinal half-car differs from the traditional half-car in pavement engineering, as it considers the two axles of the vehicle. The DOFs represent the mass pitch rotation (θ_s), the bounce displacement (v_s) and the two axle displacements ($v_{u,1}$; $v_{u,2}$). The Winkler

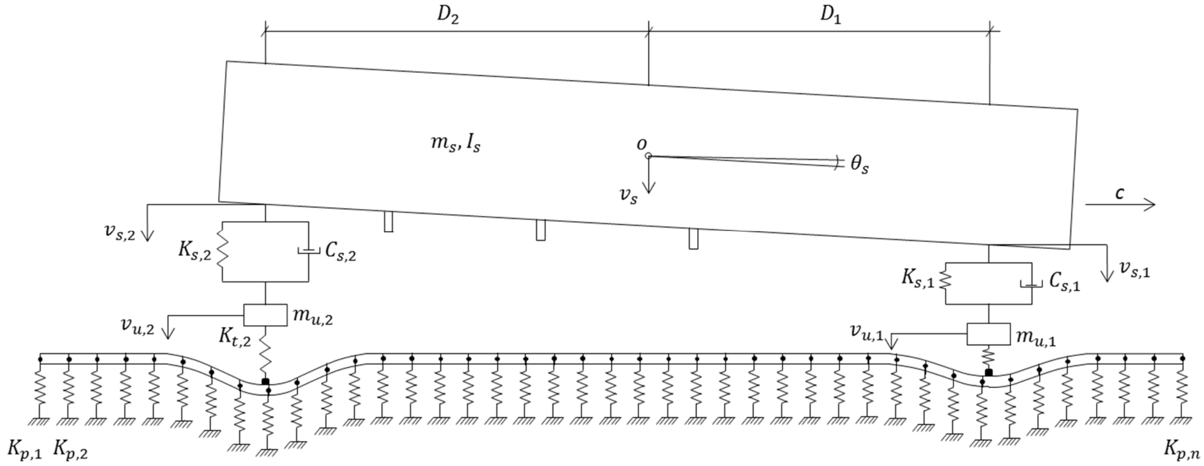

Figure 4. Half-car model passing over a Winkler model

model with the half-car is shown in Figure 4.

Values for elastic modulus in asphalt pavements are between 1 and 3 GPa and it is usually taken to be 3 GPa (De Beer et al., 1989). Here, the model properties of Table 1 have been adopted. Boussinesq theory is considered with no depth in the road pavement and loads applied in the top plane. Tyre stiffness and damping are extracted from the literature (Cebon, 1999). A double tyre in the rear axle is considered. The properties of the half-car model are given in Table 2.

Table 1. Winkler model parameters for asphalt road pavement

Pavement Model Property	Value
Number of beam elements per meter	5
Number of springs per meter	5
Spacing between springs	0.2 m
Length of the beam	50 m
Mass per unit length	2500 kg/m
Beam Damping	3%

Table 2. Half-Car model parameters

Half-Car Model Property	Value
Mass of the sprung mass	10 t
Unsprung mass axle 1	500 kg
Unsprung mass axle 2	500 kg
Length of the vehicle	11.25 m
Axle spacing	7.6 m
Tyre 1 stiffness	4×10^5 N/m
Tyre 2 stiffness	1×10^6 N/m
Suspension 1 stiffness	1.75×10^6 N/m
Suspension 2 stiffness	3.5×10^6 N/m
Suspension 1 damping	1×10^4 Ns/m
Suspension 2 damping	2×10^4 Ns/m
Centre of gravity distance from Axle 1	5.7 m
Centre of gravity distance from Axle 2	1.9 m
Axle load in Axle 2	8×10^4 N
Height of the vehicle	3.76 m
Constant velocity	72 km/h (20 m/s)

The TSD is simulated to pass over four segments of pavement with different stiffness properties. The deflection basins are estimated using the numerical simulation obtained in the Winkler model (Fig. 5). Fatigue damage is considered in this model assuming the origin of the crack at the bottom of the asphaltic layer (Cebon, 1999). Reduced stiffness can be calculated as follows (Collop and Cebon, 1995):

$$\frac{K}{K_0} = exp^{-C_3 D} \tag{6}$$

where K is the damaged stiffness, C_3 is a constant and D is a number related to the number of cycles needed to the failure. If the stiffness ratio is less than 0.2 the pavement is considered to have failed (Taheri et al., 2012). Therefore, the crack is simulated as a loss of stiffness in both beam and spring of 30%, equivalent to a stiffness ratio of 0.7, between 20 and 22 m. No delay of the maximum deflection point is considered.

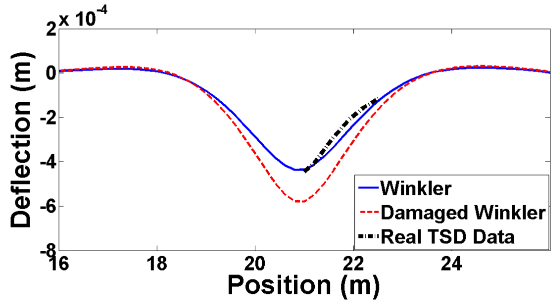

a) $K_p = 1.6 \times 10^7$ N/m ; $E = 3.6 \times 10^7$ N/m^2

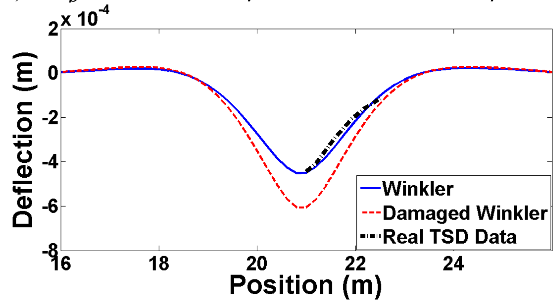

b) $K_p = 1.7 \times 10^7$ N/m ; $E = 2.6 \times 10^7$ N/m^2

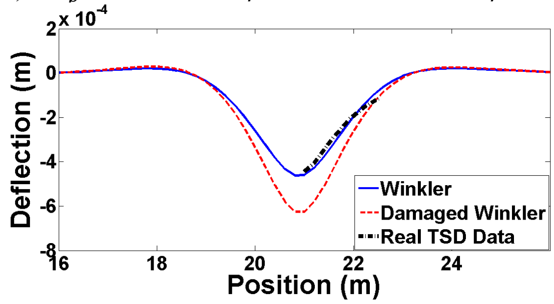

c) $K_p = 1.8 \times 10^7$ N/m ; $E = 2.0 \times 10^7$ N/m^2

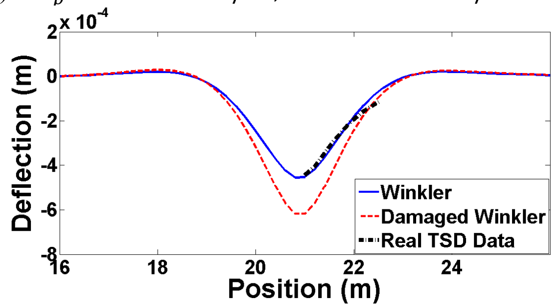

d) $K_p = 1.9 \times 10^7$ N/m ; $E = 1.8 \times 10^7$ N/m^2

Figure 5. One TSD-measured deflection basin compared to the Winkler model with 4 different value sets of spring stiffness (K_p) and beam stiffness (EI).

The results are compared to measurements obtained from a TSD passing over an asphalt pavement in South Carolina (EEUU) the 15th of July 2015. The mean values of the TSD measurements over 319.5 m at every sensor location are used. In Figure 5, four different cases varying the stiffness of the springs (K_p) and the beam stiffness (EI) are shown and used based on the TSD real measurements. Figure 5a shows the simulated basin of a pavement with low spring stiffness and a relatively high beam elastic modulus. In this situation a wider deflection basin is obtained due to a greater sharing of load between the springs. Using the parameters shown in Figure 5a, the extremes of the deflection basin can be modelled more accurately. In figures 5b and 5c intermediate quantities of both stiffnesses are applied to the model. A good approximation to the real data is obtained with this model in the extremes and in the maximum value of the deflection basin. In figure 5d the best approximation to the maximum deflection can be obtained compared to the previous cases, but lower accuracy in the extreme part of the deflection basin is achieved. In all the graphs the damage modelled is proportional to the undamaged situation.

It is shown that all the numerical models of Figure 5 can be an acceptable approximation of a real TSD in a shape comparison. A better approach to the real measurements is obtained varying the two variables that simulate pavement's stiffness.

5 CONCLUSIONS

In this paper, a vehicle pavement interaction model is used to illustrate how a TSD works. A Winkler model is used to represent the pavement. Combining the two main parameters to define the model, beam stiffness and spring stiffness, an approximation of the behaviour of the pavement can be obtained. Damage behaves proportional to the undamaged situation. The pavement deflections are calculated from the TSD measurements and compared to numerical model. It is shown the numerical model provides the deflections with an acceptable accuracy. However, more complex models are needed to consider the multiple layers of a pavement in order to separate the influence of damage in the different layers. It is suggested that the TSD measurements are carried on a road with known soil characteristics in future studies.

6 ACKNOWLEDGEMENTS

The authors acknowledge the support for the work reported in this paper from the European Union's Horizon 2020 Research and Innovation Programme under the Marie Sklodowska-Curie grant agreement No. 642453. Greenwood Engineering, designers of the TSD, are also acknowledged for their cooperation and support.

7 REFERENCES

CEBON, D. 1999. *Handbook of vehicle-road interaction,* Lisse, Swets and Zeitlinger.

CHANG, J.-R., LIN, J.-D., CHUNG, W.-C. & CHEN, D.-H. 2002. Evaluating the structural strength of flexible pavements in Taiwan using the falling weight deflectometer. *International Journal of Pavement Engineering,* 3**,** 131-141.

CHOU, Y. & LYTTON, R. L. 1991. Accuracy and consistency of backcalculated pavement layer moduli. *Transportation Research Record***,** 62-75.

COLLOP, A. & CEBON, D. 1995. A model of whole-life flexible pavement performance. *Proceedings of the Institution of Mechanical Engineers, Part C: Journal of Mechanical Engineering Science,* 209**,** 389-407.

DAVIES, T. G. & MAMLOUK, M. 1985. Theoretical response of multilayer pavement systems to dynamic nondestructive testing. *Transportation Research Record***,** 1-7.

DE BEER, M., HORAK, E. & VISSER, A. T. 1989. *The multidepth deflectometer (MDD) system for determining the effective elastic moduli of pavement layers*, ASTM International.

DE VELASCO, M. G. & MCCULLOUGH, B. F. 1983. Rigid pavement network rehabilitation scheduling using distress quantities. Texas.

DONOVAN, P. & TUTUMLUER, E. 2009. Falling weight deflectometer testing to determine relative damage in asphalt pavement unbound aggregate layers. *Journal of the Transportation Research Board***,** 12-23.

GOPALAKRISHNAN, K. & KHAITAN, S. K. 2010. Finite element based adaptive neuro-fuzzy inference technique for parameter identification of multi-layered transportation structures. *Transport,* 25**,** 58-65.

JOHNSON, R. F., BONDURANT, P. D. & MARVIN, M. H. 1996. A Rolling Weight Deflectometer for Quantitative Pavement Measurements. *In:* THOMPSON, D. O. & CHIMENTI, D. E. (eds.) *Review of Progress in Quantitative Nondestructive Evaluation: Volume 15A.* Boston, MA: Springer US.

KATICHA, S. W., BRYCE, J., FLINTSCH, G. & FERNE, B. 2014a. Estimating "True" Variability of Traffic Speed Deflectometer Deflection Slope Measurements. *Journal of Transportation Engineering,* 141.

KATICHA, S. W., FLINTSCH, G., BRYCE, J. & FERNE, B. 2014b. Wavelet denoising of TSD deflection slope measurements for improved pavement structural evaluation. *Computer-Aided Civil and Infrastructure Engineering,* 29**,** 399-415.

RADA, G. R., NAZARIAN, S., VISINTINE, B. A., SIDDHARTHAN, R. V. & SIVANESWARAN, N. 2015. Use of High-Speed Deflection Devices in Network-Level PMS Applications: Are We Ready? *In:*

DIEFENDERFER, B. & KATICHA, M. (eds.) *9th International Conference on Managing Pavement Assets.* Alexandria, Virginia, EEUU.

RASMUSSEN, S., KRARUP, J. A. & HILDEBRAND, G. 2002. Non-contact deflection measurement at high speed. *In:* TUTUMLUER, E. & AL-QADI, I. L. (eds.) *The 6nd International Conference on the Bearing Capacity of Roads, Railways and Airfields.* Lisbon, Portugal: CRC Press, Taylor and Francis Group.

ROESSET, J. M. & SHAO, K.-Y. 1985. *Dynamic interpretation of dynaflect and falling weight deflectometer tests*, Transport Research Board.

SHAHIN, M. Y. & KOHN, S. D. 1981. Pavement maintenance management for roads and parking lots. Champaign, Illinois: Construction Engineering Research Lab (Army).

SHAHIN, M. Y. & WALTHER, J. 1990. Pavement maintenance management for roads and streets using the PAVER system. Champaign, Illinois: Construction Engineering Research Lab (Army).

TAHERI, A., OBRIEN, E. & COLLOP, A. 2012. Pavement Damage Model Incorporating Vehicle Dynamics and a 3-Dimensional Pavement Surface. *International Journal of Pavement Engineering,* 12**,** 374-383.

VON QUINTUS, H. & KILLINGSWORTH, B. 1997. Design pamphlet for the backcalculation of pavement layer moduli in support of the 1993 AASHTO Guide for the Design of Pavement Structures. Federal Highway Administration.

XU, B., RANJI RANJITHAN, S. & RICHARD KIM, Y. 2002. New relationships between falling weight deflectometer deflections and asphalt pavement layer condition indicators. *Transportation Research Record: Journal of the Transportation Research Board***,** 48-56.

YI, J. H. & MUN, S. 2009. Backcalculating pavement structural properties using a Nelder–Mead simplex search. *International journal for numerical and analytical methods in geomechanics,* 33**,** 1389-1406.